Journal of Thermal Analysis and Calorimetry, Vol. 55 (1999) 949-975

PHYSICAL AGING OF MALTOSE GLASSES AS MEASURED BY STANDARD AND MODULATED DIFFERENTIAL SCANNING CALORIMETRY

A. M. Lammert[1], *R. M. Lammert*[2] *and S. J. Schmidt*[3*]

[1]Hunt-Wesson, Inc., 1645 W. Valencia Dr., Fullerton, CA 92833-3899
[2]Ortel Corporation, 2015 W. Chestnut St., Alhambra, CA 91803-1542
[3]Department of Food Science and Human Nutrition, 905 S. Goodwin Ave., Urbana, IL 61801 USA

(Received April 21, 1998)

Abstract

The physical aging characteristics of maltose glasses aged at two temperatures below the glass transition temperature, T_g, (T_g 10°C and T_g 20°C) from 5 to 10 000 min were measured by standard differential scanning calorimetry (SDSC) and modulated differential scanning calorimetry (MDSC). The experimentally measured instrumental T_g, the calculated T_g, and the excess enthalpy values were obtained for aged glasses using both DSC methods. The development of excess enthalpy as a function of aging time, as measured by both SDSC and MDSC, was fit using the Cowie and Ferguson and Tool-Narayanswamy-Moynihan models. The change in the T_g values and the development of the excess enthalpy resulting from physical aging measured by the two DSC methods are discussed.

Keywords: modulated DSC, physical aging, standard DSC

Introduction

A material in the glassy state is regarded as a solidified, supercooled liquid whose volume, enthalpy, and entropy are greater than they would be in the equilibrium condition [1]. Some properties of the material in this nonequilibrium condition continue to undergo relative slow relaxation over time, attempting to obtain equilibrium, even at temperatures well below their glass transition temperature (T_g) without the influence of any external factors or forces. This gradual continuation of the glass formation that occurs below T_g is referred to as physical aging and occurs in a similar manner for all synthetic and natural materials [1].

* Author for correspondence: phone: (217)333-1324; email: sjs@uiuc.edu

1418–2874/99/ $ 5.00

Akadémiai Kiadó, Budapest
Kluwer Academic Publishers, Dordrecht

Physical aging is also referred to as structural relaxation, volume recovery, volume relaxation, enthalpic recovery, or enthalpic relaxation. Physical aging results in changes of material properties such as length, hardness, brittleness, density, enthalpy, creep- and stress-relaxation rates, dielectric constant and dielectric loss.

The importance of understanding the process of physical aging of food materials has just begun to be appreciated, as demonstrated by its more recent appearance in the foods, pharmaceutical, and biological literature [2–6]. The importance of enthalpic relaxation has been recognized for carbohydrates [7–10], proteins [11] and intact food systems [12, 13]. To date, the physical aging of only a few food ingredients, such as sucrose [1, 14, 15], maltose [16], starch [7, 17–22], and acetic acid soluble wheat gluten [23] and one intact food system, cheese [1], have been systematically studied.

Schmidt and Lammert [16] examined the physical aging characteristics of maltose glasses using a SDSC instrument. An amorphous maltose glass was made by melting crystalline maltose in a hermetically sealed DSC pan and the molten maltose was then quench cooled to the aging temperature, 30°C (approximately 12°C below the T_g). The maltose glass was aged from 5 min to 10 days in a Mettler DSC instrument. After the material was aged, the maltose was quench cooled to –20°C, scanned at a rate of 10°C min^{-1} to 140°C (aged scan), quench cooled to –20°C, and rescanned at a rate of 10°C min^{-1} to 140°C (unaged rescan – the prior thermal history was erased when the maltose glass was heated above its T_g in the aged scan). The difference in enthalpy (or excess enthalpy) between the aged and unaged glass was obtained by subtracting the unaged rescan from the aged scan. The T_g values obtained by the instrument software were found to increase slightly with aging time, whereas the T_g calculated values (the intersection of the enthalpy-temperature lines for the glass and liquid states obtained using the method of Richardson and Savill [24] were found to decrease with aging time. Since the aged maltose glass is relaxing toward equilibrium, it is expected that the T_g calculated would decrease. The amount of excess enthalpy increased with longer aging times up to approximately 1000 min and then leveled off indicating that the material was nearing equilibrium.

MDSC is a new technique that differs from SDSC by superimposing a sinusoidal modulation on the linear heating rate, resulting in a sinusoidal heating rate instead of a linear heating rate [25]. In essence, there are two heating rates, a constant one (the underlying linear heating rate) and a sinusoidal one (the instantaneous heating and cooling rate imposed by the modulation conditions). There are two advantages of MDSC: 1. improved sensitivity and resolution for the detection of transitions and 2. separation of reversing events, such as the glass transition, from nonreversing events, such as physical aging. MDSC has been shown to separate the effects of physical aging from the glass transition of polystyrene [26, 27]. To date, only a few publications using MDSC are available in the food science literature at the time this introduction was written [28–30].

The objectives of this research were: 1) to measure the change in the experimentally measured instrumental T_g, the calculated T_g, and the excess enthalpy values that result from the process of physical aging in maltose glasses using SDSC and MDSC at aging temperatures of 23°C (approximately 14°C below T_g midpoint) and 13°C (approximately 24°C below T_g midpoint) for SDSC and 20°C (approximately 13°C below T_g midpoint) and 10°C (approximately 23°C below T_g midpoint) for MDSC as a function of aging time (from 5 to 10 000 min) and 2) to model the development of enthalpic relaxation as a function of aging time using both the Cowie and Ferguson (CF) and Tool-Narayanaswamy-Moynihan (TNM) models.

Materials and methods

Materials

Grade I maltose monohydrate (4-O-α-*D*-glucopyranosyl-*D*-glucose) was obtained from Sigma Chemical Company (St. Louis, MO) and used without further purification. The moisture content of the maltose was determined by Karl Fisher Titration [31] and is 5.174±0.0058% (wet basis), based on duplicate measurements.

Static was prevented from forming during the preparation of the maltose samples by: 1) using a Kimwipe sprayed with AntiStatic spray (Richland Research Co., Scottsdale, AZ) to wipe the outside of the maltose container and 2) grounding all of the utensils.

Instrument

A TA Instruments 2920 MDSC, equipped with a refrigerated cooling accessory, and Thermal Solutions Instrument Control and RMX software (for SDSC) and Universal Analysis software (for MDSC) was used. For both SDSC and MDSC measurements, dry He gas was purged through the sample cell at a rate of 25 $cm^3\ min^{-1}$. Dry N_2 gas was purged through the refrigerated cooling accessory during heating and dry He gas was used for cooling; both were at a rate of 150 $cm^3\ min^{-1}$.

Sample preparation

The maltose samples (6.50±0.25 mg) were weighed into acetone washed, unmodified, coated aluminum DSC pans (900760.901, pan, and 900970.901, lid, TA Instruments, Inc., New Castle, DE) and hermetically sealed. The DSC pans were sonicated in acetone for 30 min to remove any residual machine oil that may have remained on them from the manufacturing process. The DSC pans were removed from the acetone, wrapped in paper towels, and allowed to dry at

room temperature overnight. For maximum temperature control, the amorphous maltose glasses were made and aged in the instrument.

Calibration

The instrument was calibrated using indium (900902.901, TA Instruments, Inc., New Castle, DE). Sapphire (915079.902, TA Instruments, Inc., New Castle, DE) was used as the heat capacity standard. For MDSC, the sapphire standard was run using the steady state conditions determined for maltose (described below). An empty, acetone washed, unmodified, sealed coated aluminum DSC pan was used as the reference pan in all measurements and both the reference and sample pans were matched in mass to within ±0.10 mg.

MDSC steady state conditions

The temperature amplitude, A_T, and period, p, are two additional parameters in MDSC, not used in SDSC, that control the height and width, respectively, of the sinusoidal heating rate. In MDSC, it is important for the sample to achieve steady state heat capacity because this condition is needed in order for the sample to follow the imposed modulation conditions [32]. Steady state heat capacity is achieved when the heat capacity of a material does not change with p at a constant A_T.

The steady state conditions of an amorphous maltose glass (the glass was formed as outlined below, steps a and b) were determined quasi-isothermally (underlying heating rate=0°C min^{-1}) at two temperatures, one below the T_g (−10°C) and one above the T_g (90°C) of the material. The modulation conditions used were A_T of 0.5°C and p of 60, 70, 80, 90, and 99 s. A 100 second period was not used because it is the upper limit of the instrument and often resulted in a distorted modulated signal. The sample was held at each modulation conditions for 20 min. The first 10 min were used to equilibrate the sample to the imposed modulation conditions and the last 10 min were used for data collection. The steady state conditions for maltose at −10 and 90°C were obtained at a p of 80 s and greater. In order to ensure that steady state conditions were obtained, an A_T and p of 0.5°C and 99 s, respectively, were used in the MDSC experiments.

A mathematical description of the separation of the reversing (i.e. T_g) and nonreversing (i.e. enthalpic relaxation) events by MDSC is given by Wunderlich *et al.* [33]. For sufficient separation of the reversing and nonreversing events, 4 to 5 modulation cycles per glass transition region (T_g onset to T_g endpoint) are suggested [32]. Since the T_g region of an unaged maltose glass is approximately 6–10°C, these experiments were done at an underlying heating rate of 1°C min^{-1}. The number of modulation cycles per glass transition region of an unaged maltose glass measured by MDSC in this experiment was 3.5. In order to get 4 or more modulation cycles per glass transition region, the modulation period

would have to be decreased. Unfortunately, a decreased modulation period resulted in a faster instantaneous heating and cooling rate and the sample was not be able to follow the modulation conditions imposed causing a loss of steady state conditions.

Thermal history

The thermal history employed in this study is similar to that used by Montserrat [34] for epoxy resins and is outlined below (a through e). Figure 1 is the schematic representation of the corresponding changes in enthalpy as experienced by the samples during the thermal treatment.

a) The maltose sugar crystals were melted in the DSC pan by increasing the temperature from room temperature to 140°C at a rate of 10°C min^{-1}. The sample was held at 140°C for four min to ensure complete melting ($m.p.$=136°C) of the maltose crystals (molten maltose, Fig. 1, A).

b) The molten sugar sample was then cooled (10°C min^{-1} SDSC; 1°C min^{-1} MDSC) to –20°C for the unaged SDSC and MDSC samples or to the aging temperature (SDSC: 23 or 13°C and MDSC: 20 or 10°C, these aging temperatures are approximately equal to [T_g onset –20°C] and [T_g onset –10°C]). For MDSC, no modulation was done during cooling. This step forms the amorphous glass (path AB). For the unaged SDSC and MDSC samples, steps c and d were omitted.

c) The sample was then held at the aging temperature (T_a) for various aging times (t_a; 5 to 10 000 min). Short aging time measurements (5 to 360 min) were done in duplicate, whereas single values were obtained for aging times greater than 360 min. This isothermal aging process is represented by the decrease in enthalpy from point B to C in Fig. 1.

d) At the end of the aging time, the sample was cooled (10°C min^{-1} SDSC; 1°C min^{-1} MDSC, without modulation) to –20°C (path CY).

e) For the SDSC, the sample was immediately scanned from –20 to 140°C at a rate of 10°C min^{-1} (path YCA). This SDSC scan will be referred to as the aged SDSC curve. For the MDSC, the sample was held isothermally at –20°C for 10 min while the imposed modulation conditions (A_T=0.5°C and p=99 s) were allowed to equilibrate. After which, the sample was immediately scanned from –20 to 140°C at a rate of 1°C min^{-1} in the MDSC (path YCA). Unequal heating and cooling rates are known to affect the T_g and the enthalpic behavior of a material [35]. Thus, equal heating and cooling rates were used within in both SDSC (10°C min^{-1}) and MDSC (1°C min^{-1}) experiments to minimize this effect.

An additional curve for SDSC on the same sample is needed to quantitate the amount of energy associated with the enthalpic relaxation. The scan was done by cooling (10°C min^{-1} SDSC) the sample in step (e), above, to –20°C and rescanning to 140°C at 10°C min^{-1} (path ABXBA in Fig. 1). This DSC scan will be re-

ferred to as the unaged rescan SDSC curve. It is important to note that in order to obtain the unaged rescan SDSC curve using the same sample, the previous thermal history of the 'aged' sample was erased by heating the sample to 140°C in step (e). An additional MDSC curve was not needed since MDSC separates the reversing and nonreversing events and the enthalpic relaxation can be determined directly from the nonreversing MDSC curve (described below); thus, no rescan was done for the MDSC experiments.

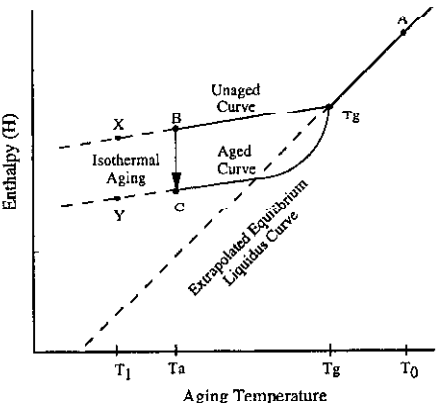

Fig. 1 Schematic diagram of the enthalpy changes in a maltose glass subjected to the unaged or aged thermal histories described in the text for SDSC or MDSC. The unaged path is ABXBA and the aged path ABCYCA

Heat capacity values, as a function of temperature, were measured for unaged, aged, and unaged rescan maltose glasses in order to obtain the T_g calculated values. Heat capacity values for amorphous maltose were obtained in SDSC between 0 and 90 at 2°C intervals for both the aged and unaged samples. Unlike SDSC, MDSC can measure the heat capacity of a material during the measurement; therefore, heat capacity values for amorphous maltose measured were obtained between –20 and 140°C.

Determination of T_g values

The glass transition values were determined using the RMX software for SDSC and the Universal Analysis software for MDSC. For both SDSC and MDSC the glass transition values obtained were: T_g onset – the intersection of the regression line from the start with the inflection tangent of the step change; T_g midpoint – the point where the transition of the sample is 50% complete; and T_g endpoint – the intersection of the inflection tangent with the regression line after the transition [37].

In addition, T_g was calculated for the unaged and aged curves from SDSC and the aged curve from MDSC as the intersection of the enthalpy-temperature lines

for the glass and liquid states, using the method of Richardson and Savill [24]. The enthalpy-temperature lines were obtained by integrating the heat capacity-temperature lines in the glass and liquid regions.

Enthalpy measurements

The difference in enthalpy (ΔH, J g^{-1}) between the aged and the unaged rescan maltose samples in SDSC was obtained according to the procedure given by Montserrat [34]. ΔH can be calculated using Eq. (1) [38]:

$$\Delta H = \int_{T_1}^{T_0} (C_{P_{aged}} - C_{P_{unaged}}) dT \quad (1)$$

where $C_{P_{aged}}$ and $C_{P_{unaged}}$ are the specific heats of the aged and unaged samples, respectively, and T_1 and T_0 are the temperatures shown in Fig. 1. Based on the principles of SDSC, the output power P is directly proportional to the C_p of the sample, $C_p = P/q^* m$), where m is the dry mass of the sample and q is the heating rate. If we assume that the sample is heated at the same rate as the furnace, the relaxation enthalpy can be calculated by subtracting the unaged rescan SDSC power curve from the aged SDSC power curve and integrating the difference in area between the two curves using Eq. (2):

$$\Delta H = \frac{1}{m} \int_{t_1}^{t_0} (P_{aged} - P_{unaged}) dt \quad (2)$$

where m is the dry mass of the sample, P_{aged} and P_{unaged} are the output powers for the aged and unaged rescan SDSC scans, respectively, and t_1 and t_0 are the times corresponding to temperatures T_1 and T_0 in Fig. 1, respectively. In practice, due to noise in the baseline of the DSC curves, temperatures (Eq. (1)) and times (Eq. (2)) close to the area to be integrated are used.

An example of an MDSC curve for a maltose glass aged for 360 min at 20°C is shown in Fig. 2. Since MDSC separates the glass transition (reversing heat flow curve – Fig. 2a) from the enthalpic relaxation (nonreversing heat flow curve

Table 1 Integration limits used to obtain the $\Delta H(t)$ values in SDSC and MDSC at the different aging temperatures

DSC type$_{\text{aging temperature}}$/°C	Integration limits/°C
SDSC–23	20–55 & 25–50
SDSC–13	18–60 & 20–62
MDSC–20	20–60 & 25–55
MDSC–10	19–45 & 20–44

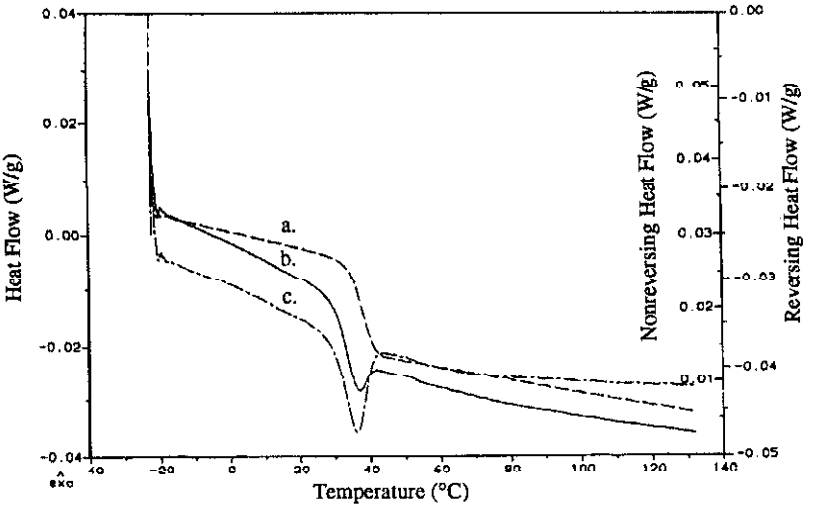

Fig. 2 A MDSC curves of a maltose glass aged for 360 min at 20°C. The curves was obtained with an underlying heating rate of 1°C min^{-1}, A_T=0.5°C and p=99 s. a) Reversing Heat Flow, b) Total Heat Flow, c) Nonreversing Heat Flow

– Fig. 2c), there is no need to subtract the unaged rescan from the aged curve described above for SDSC. Excess enthalpy, ΔH, values were obtained by integrating the area under the nonreversing curve near the glass transition region.

Cowie and Ferguson [38] found the choice of the two integration limits can influence the value of ΔH that is obtained. To minimize this effect, two sets of reasonable integration limits were selected as determined by inspecting several curves for both SDSC and MDSC. The integration limits for SDSC and MDSC are given in Table 1. In addition, three randomly selected pairs of integration limits between these values were selected. Thus, each ΔH value is the average of five integration areas.

Results and discussion

T_g values obtained from SDSC and MDSC

Unaged maltose glasses

The T_g values were measured using two methods: the instrument software and by calculation. T_g onset, T_g midpoint, and T_g endpoint obtained from the instrument software and T_g calculated for unaged maltose glasses measured by SDSC and MDSC can be found in Table 2.

The differences in the maltose T_g values measured by the SDSC heat flow and the MDSC total heat flow may be attributed to the different heating and cooling rates at which they were measured. The heating and cooling rate are known to af-

Table 2 The glass transition and ΔC_p values of unaged amorphous maltose prepared from maltose monohydrate. The T_g onset, T_g midpoint, and T_g endpoint were obtained from SDSC using the RMX software. The T_g onset, T_g midpoint, and T_g endpoint were obtained from the total heat flow and reversing heat flow for MDSC using the Universal Analysis software. The T_g calculated and ΔC_p values were obtained using the method of Richardson and Savill [24]

SDSC–heat flow	Unaged T_g or ΔC_p value
T_g onset	33.80±0.06°C
T_g midpoint	37.36±0.08°C
T_g endpoint	41.32±0.15°C
SDSC–heat capacity	
T_g calculated	34.43±0.96°C
ΔC_p	0.60±0.01 J $g^{-1}K^{-1}$
MDSC–total heat flow	
T_g onset	30.19±0.85°C
T_g midpoint	33.16±0.71°C
T_g endpoint	36.04±0.71°C
MDSC–reversing heat flow	
T_g onset	33.82±0.69°C
T_g midpoint	37.56±0.51°C
T_g endpoint	41.39±0.46°C
MDSC–heat capacity	
T_g calculated	37.24±0.40°C
ΔC_p	0.60±0.01 J $g^{-1}K^{-1}$

fect the T_g [35, 39]. The solver the cooling rate, the lower the temperature at which the enthalpy curve departs from the equilibrium liquidus curve and begins the non-equilibrium glassy curve. The MDSC cooling rate (1°C min^{-1}) was solver than the SDSC cooling rate (10°C min^{-1}) and the T_g values obtained from MDSC total heat flow were lower than those obtained from SDSC. The T_g values obtained from the reversing heat flow of MDSC are similar, but slightly higher than the values obtained from the heat flow of SDSC. Boller *et al.* [26] found the T_g of polystyrene obtained from the reversing heat flow of MDSC was not affected by the prior thermal history or the heating and cooling rate; however, the T_g value of polystyrene decreased by 2°C when the period of modulation was increased by a factor of three at a constant instantaneous heating and cooling rate of 3.8°C min^{-1}. Jin *et al.* [40] found a significant difference in the cold crystal-

lization temperature of poly(butylene terephthalate) and polycarbonate blends obtained by SDSC and MDSC indicating that the total heat flow obtained by MDSC may not be the same as the heat flow obtained by SDSC.

The T_g calculated obtained for unaged maltose glasses for SDSC was between the T_g onset and T_g midpoint of the heat flow T_g values. The T_g calculated was also between the T_g onset and T_g midpoint for the MDSC reversing heat flow; however, when compared to the MDSC total heat flow, the MDSC T_g calculated was greater than the T_g endpoint.

ΔC_p values for unaged maltose glasses measured by SDSC and MDSC are given in Table 2. The ΔC_p values obtained were similar to those found by Roos [41] and Schmidt and Lammert [16] at 0.61 and 0.62 J g^{-1} K^{-1}, respectively, but lower than the value of 0.79 J g^{-1} K^{-1} reported by Orford *et al.* [42].

A 'true' unaged maltose glass was not able to be measured by MDSC. Since a slow heating and cooling rate (1°C min^{-1}) was used and the sample was held at −20°C for 10 min to equilibrate the modulation conditions, the 'unaged' sample was actually aged as it was being cooled, equilibrated (isothermally for 10 min for the modulation conditions to equilibrate), and reheated during the measurement method. Physical aging was evident by the enthalpic relaxation present in the nonreversing and total heat flow MDSC curves of an 'unaged' maltose glass.

The 'unaged' maltose T_g onset, midpoint, and endpoint values obtained from the MDSC total heat flow are 3.63, 4.40 and 5.35°C less, respectively, than the T_g onset, midpoint, and endpoint values obtained from the MDSC reversing heat flow. The difference between the MDSC total heat flow and the MDSC reversing heat flow is an estimate of the effect of the enthalpic peak on the instrument software measurement of T_g.

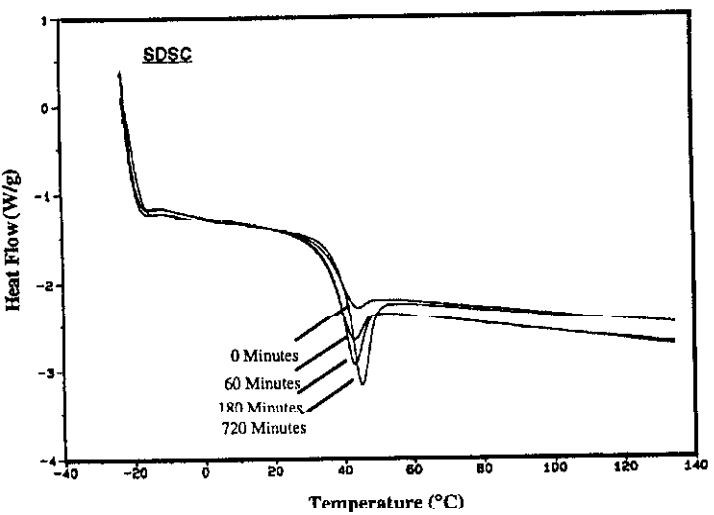

Fig. 3 SDSC curves of an unaged and three maltose (60, 180 and 720 min) glasses aged at 23°C prepared and aged as illustrated in Fig. 1

Aged maltose glasses

Typical SDSC curves for an unaged and three aged maltose glasses are shown in Fig. 3 and typical MDSC total heat flow curves for an 'unaged' and three aged maltose glasses are shown in Fig. 4. The difference in the heat flow between Figs 3 and 4 is due to the difference in the heating rate used. The glass transition values were also determined for the aged maltose glasses by the two methods discussed above (the instrument software and by calculation). The T_g values obtained were plotted as a function of the log of the aging time and are shown in Figs 5–7 for the heat flow from SDSC, total heat flow from MDSC, and reversing heat flow from MDSC, respectively.

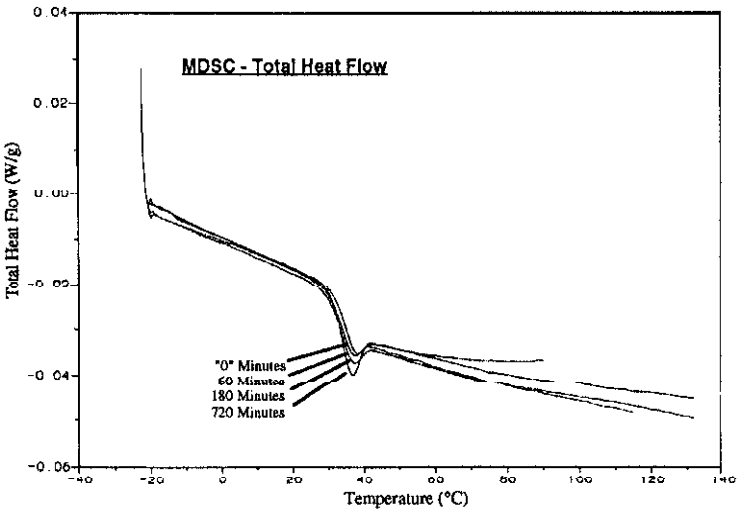

Fig. 4 MDSC curves (from the total heat flow) of an unaged and three maltose (60, 180 and 720 min) glasses aged at 20°C prepared and aged as illustrated in Fig. 1

For maltose glasses aged at 23°C and measured by SDSC (Fig. 5), there was a slight overall increase in the T_g values as a function of aging time and a narrowing of the glass transition region (T_g onset to T_g endpoint) from 6.75°C, at an aging time of 5 min, to 1.57°C, at an aging time of 10 000 min. For maltose glasses aged at 13°C and measured by SDSC (Fig. 5), a slight decrease in the T_g values and an overall narrowing of the glass transition region was found for aging times between 50 to 1000 min. For maltose glasses aged at 20°C and measured by the MDSC total heat flow (Fig. 6), the T_g onset and T_g midpoint values were constant until an aging time of 1000 min and then began to increase, whereas the T_g endpoint decreased until an aging time of 1000 min and then began to increase. The T_g region also narrowed from 5.83°C at an aging time of 5 min to 1.50°C at an aging time of 10 000 min. For maltose glasses aged at 10°C and measured by the MDSC total heat flow (Fig. 6), the T_g onset and T_g midpoint values were con-

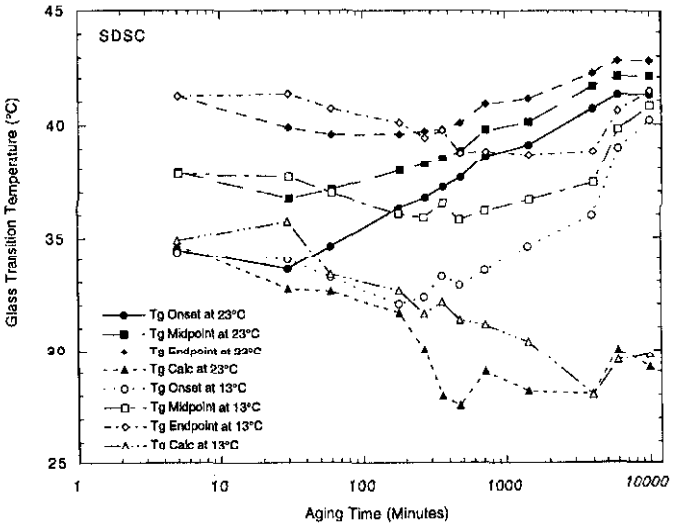

Fig. 5 T_g values (T_g onset, T_g midpoint and T_g endpoint) for maltose glasses measured by SDSC, plotted as a function of log of aging time at two aging temperatures, 23 and 13°C. The T_g calculated was determined from the heat capacity values measured by SDSC

stant, but showed some variability, whereas the T_g endpoint was constant until an aging time of 1000 min and then it started to decrease. In addition, a slight narrowing of the T_g region was observed. For maltose glasses aged at 20°C and measured by the MDSC reversing heat flow (Fig. 7), the T_g values remained constant until an aging time of 1000 min and then began to increase and the T_g region narrow slightly. For maltose glasses aged at 10°C and measured by the MDSC reversing heat flow (Fig. 7), the T_g values did not change, but did show some variability.

The difference between the T_g values for maltose glasses aged at the two different temperatures below T_g by both DSC methods is due to the solver relaxation toward equilibrium that occurs at aging temperatures further below T_g. The increase in the T_g values with aging time is well established [43] and has been observed for synthetic polymers such as polyesters [44], polyetherimide [45], polyvinyl chloride [46], and polyethylene terephthalate [47] as well as maltose [16]. However, since the reversing heat flow from MDSC should not be affected by the prior thermal history of the sample [26], the T_g values measured using the reversing MDSC heat flow curve should remain unchanged with aging time, which is what was observed for maltose glasses aged at 10°C, but not for maltose glasses aged at 20°C (Fig. 7). Figure 8 shows a decrease in the number of modulation cycles per glass transition region with an increase in aging time for maltose glasses aged at 20°C (approximately 10°C below the T_g onset) and 10°C (approximately 20°C below the T_g onset). The slight increase and narrowing observed in the T_g

values obtained from the reversing heat flow of MDSC at longer aging times (greater than 1000 min for maltose glasses aged at 20°C) may be due to the inadequate separation of the glass transition from the effects of physical aging due to the decreased number of modulation cycles per glass transition region.

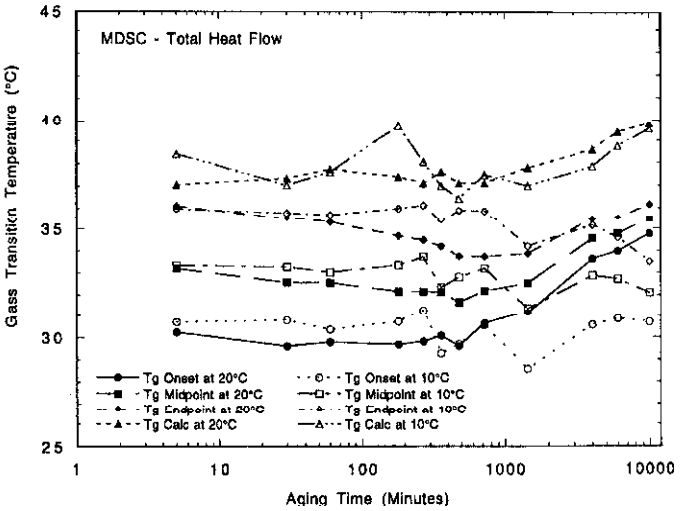

Fig. 6 T_g values (T_g onset, T_g midpoint and T_g endpoint) from the total heat flow for maltose glasses measured by MDSC, plotted as a function of log of aging time at two aging temperatures, 20 and 10°C. The T_g calculated is determined from the heat capacity values measured by MDSC

The T_g calculated value [24] is based on the intersection of the extrapolated liquid and glassy enthalpy curves at temperatures below and above the glass transition region. Since the maltose glass is relaxing toward equilibrium during the aging process (Fig. 1), it is expected that the T_g calculated would decrease with aging time. The T_g calculated values obtained from SDSC decreased with aging time for both aging temperatures (Fig. 5). However, the T_g calculated values obtained from MDSC did not decrease (Fig. 6 or 7) it remained constant at 37.59±0.83°C (the average of all unaged and aged MDSC T_g calculated values up to 720 min at aging temperatures of 20 and 10°C) until approximately 1000 min then it began to increase. The heat capacity measured by SDSC is the sum of the heat capacity of the material and the enthalpic relaxation associated with aging, whereas the heat capacity measured by MDSC is only the heat capacity of the material and does not include the effect of aging. Thus, the T_g calculated values obtained from MDSC should not decrease with aging time. However, at longer aging times (greater than 1000 min) there were not enough modulation cycles per glass transition region to separate the effect of physical aging form the glass transition and instead of remaining constant, the T_g calculated began to increase.

Tool [48] measured the change in length of aged silicate glasses at different temperatures and thermal histories and found that the structural state (and en-

thalpy changes) of an aged glass could be characterized by the fictive temperature, $T_f(t)$. $T_f(t)$ is the temperature an aged material would be at if it were instantaneously heated to the equilibrium liquidus curve [43] without a change in the enthalpy (H) of the sample. For an unaged material, the T_g is equal to the $T_f(t)$ and for an aged material at equilibrium, the $T_f(t)$ would equal the aging temperature

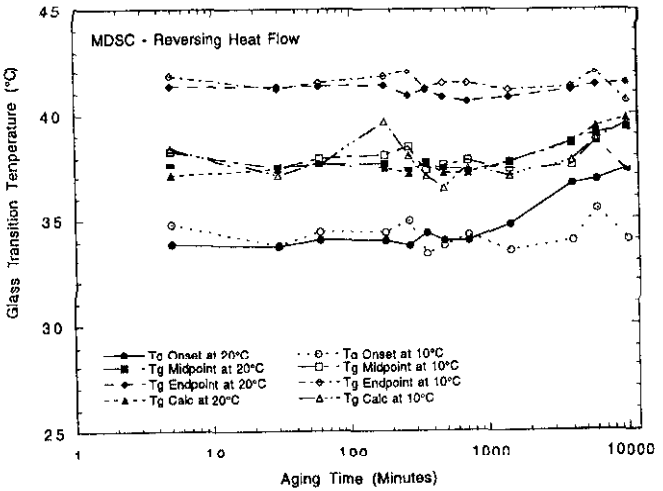

Fig. 7 T_g values (T_g onset, T_g midpoint and T_g endpoint) from the reversing heat flow for maltose glasses measured by MDSC, plotted as a function of log of aging time at two aging temperatures, 20 and 10°C. The T_g calculated is determined from the heat capacity values measured by MDSC

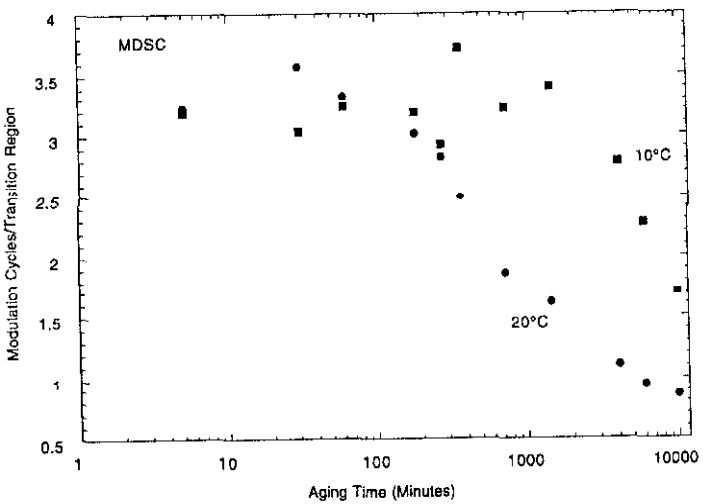

Fig. 8 The number of modulation cycles per glass transition region measured for maltose glasses aged at 20 and 10°C using MDSC

(T_a). Thus, as a material ages, the $T_f(t)$ decreases toward the extrapolated equilibrium liquidus curve. The $T_f(t)$ can be calculated using Eq. (3) [49, 50]:

$$T_f(t) = T_a + \frac{[\Delta H(\infty) - \Delta H(t)]}{\Delta C_p} \tag{3}$$

where T_a is the aging temperature (for SDSC 23 and 13°C and for MDSC 20 and 10°C), $\Delta H(\infty)$ is the excess enthalpy of an aged glass at structural equilibrium, $\Delta H(t)$ is the excess enthalpy of a glass aged at a time, t, and $\Delta C_p = C_{p_l} - C_{p_g}$, the change in heat capacity at the glass transition where l=liquid and g=glass. The $\Delta H(\infty)$ used was calculated using Eq. (5) and the ΔC_p used was 0.60 J g^{-1} K^{-1}.

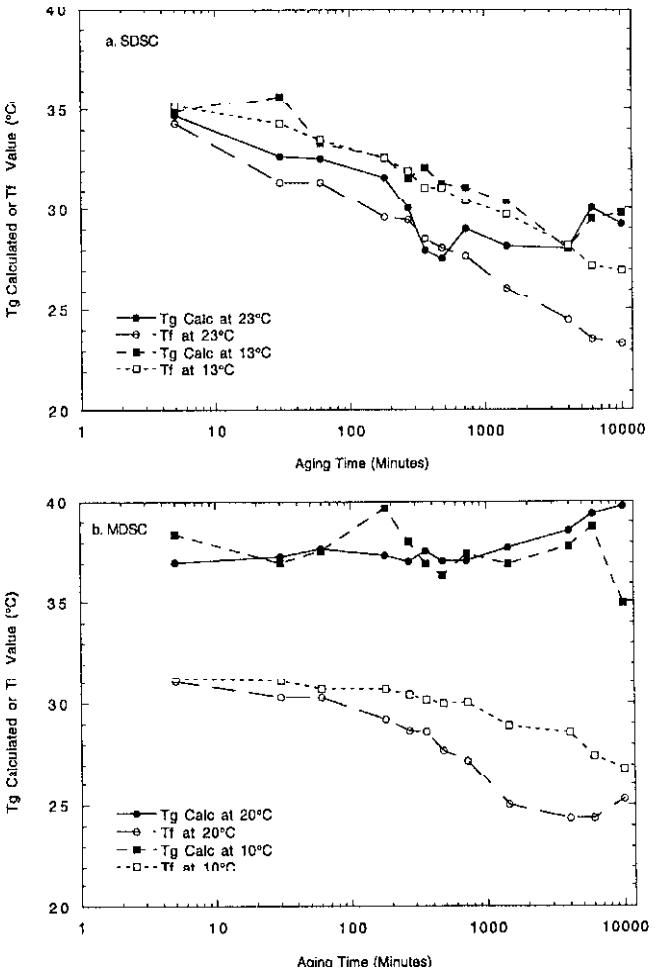

Fig. 9 T_g calculated values for aged maltose glasses compared to calculated $T_f(t)$ values. a) SDSC at two aging temperatures, 23 and 13°C, b) MDSC at two aging temperatures, 20 and 10°C

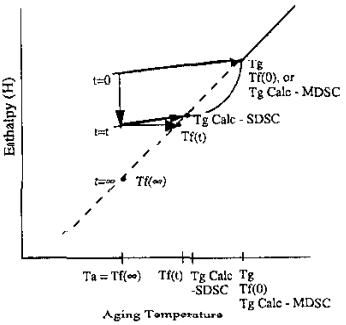

Fig. 10 A schematic diagram of the difference between $T_f(0)$, $T_f(t)$ Calc determined by SDSC and T_g Calc determined by MDSC. T_g is the glass transition temperature, T_a is the aging temperature, $T_f(0)$ is the fictive temperature at zero time, $T_f(t)$ is the fictive temperature at a time, t, $T_f(\infty)$ is the fictive temperature at $t=\infty$, T_g Calc – SDSC is the T_g Calc determined by SDSC and T_g Calc – MDSC is the T_g Calc determined by MDSC

The decrease in the $T_f(t)$ compared to the T_g calculated with aging time for maltose glasses measured by SDSC and MDSC at two aging temperatures is shown in Figs 9a and 9b, respectively. For SDSC, both the $T_f(t)$ and T_g calculated decreased with aging time at aging temperatures of 23°C and 13°C. Thus, the T_g calculated determined from SDSC measurements (finite heating rate) is similar to the $T_f(t)$ (instantaneous heating rate) as observed in Fig. 10. In the MDSC case, the situation is more complex. The $T_f(t)$ values are calculated using the nonreversing heat flow, whereas the T_g calculated values are determined using the heat capacity values. The $T_f(t)$, as measured by MDSC, decreased with aging time for aging at 20°C and slightly decreased for aging at 10°C (Fig. 9b), but the T_g calculated values were constant until an aging time of approximately 1000 min. Since the heat capacity of the material is not affected by aging in MDSC [26], the T_g calculated would not be expected to decrease and would be similar to the $T_f(0)$ or the fictive temperature of an unaged material as illustrated in Fig. 10. However, at aging times greater than 1000 min, the T_g calculated began to increase. The increase in T_g calculated may be caused by the insufficient number of modulation cycles per glass transition region needed to adequately separate the T_g from the effects of physical aging (Fig. 8). Another possible explanation for the increase in the T_g (onset, midpoint, endpoint, calculated) is local ordering or recrystallization of the maltose glasses aged longer than 1000 min. However, no melting of crystalline regions was observed in the MDSC curves for maltose glasses aged longer than 1000 min. If recrystallization did occur, it should also occur in the maltose glasses aged at 23°C measured by SDSC, but no melting or increase in T_g calculated was observed (Fig. 5). Thus, the T_g calculated may be used to indicate the relaxation toward equilibrium in aged glasses, similar to $T_f(t)$ when measured by SDSC, but it cannot be used to indicate the relaxation of aged glasses measured by MDSC.

The ΔC_p values were obtained for aged maltose glasses measured by SDSC and MDSC. No trend in the ΔC_p values with aging time was found. The ΔC_p values were averaged over all aging times for each aging temperature and are given in Table 3. ΔC_p values for aged maltose glasses obtained from this work were similar to the range of 0.58 to 0.6 J g^{-1} K^{-1} reported by Schmidt and Lammert [16] for maltose glasses aged at 30°C. The aged ΔC_p values are similar to the unaged ΔC_p values for maltose glasses measured by SDSC and MDSC in this work (Table 2).

Modeling of physical aging

Cowie and Ferguson (CF) model

The Cowie and Ferguson Model [51] uses Eq. (4) to model aging by the development of excess enthalpy:

$$\Delta H(t) = \Delta H(\infty)(1 - \varphi(t)) \tag{4}$$

where

$$\varphi(t) = \exp\left[-\left(\frac{t}{\tau}\right)^{\beta}\right] \tag{4a}$$

where $\Delta H(t)$ is the excess enthalpy of an aged glass at a time, t, $\Delta H(\infty)$ is the excess enthalpy of a material at structural equilibrium, β is a parameter used to describe the width of the relaxation time distribution spectrum ($0 \leq \beta < 1$), and τ is the characteristic aging time, also represented as t_c [51]. Equation 4a is the Williams and Watts equation [52] and is a stretched exponential function used to describe linear (only when $\beta = 1$) and nonlinear ($0 \leq \beta < 1$) relaxation events, such as physical aging. Equation 4 relates the $\Delta H(t)$ with time at a constant τ and aging temperature. The CF model can be used to obtain information about the long aging time behavior of aged polymer glasses and can be correlated to aging quantified by volumetric and mechanical methods [53, 54].

$\Delta H(\infty)$ was calculated using Eq. (5) [55]:

$$\Delta H(\infty) = \Delta C_p(T_g - T_a) \tag{5}$$

The T_g value used in Eq. (5) for SDSC was the average of all unaged rescan SDSC T_g calculated values (35.22±1.31°C). The T_g value used in Eq. (5) for MDSC was an average of all unaged and aged MDSC T_g calculated values up to 720 min at aging temperatures of 20 and 10°C (37.59±0.83°C). MDSC T_g calculated values greater than 720 min were not used because the number of modulation cycles per glass transition would not sufficiently separate reversing from nonreversing events (Fig. 8). The SDSC and MDSC ΔC_p (0.60 J g^{-1} K^{-1}) for

unaged maltose glasses listed in Table 1 were used. τ and β were determined using a nonlinear least squares fit to Eq. (4) using the solver function in Microsoft Excel and minimized using Eq. (6).

$$SS = \sum_{I} (\Delta H(t)_{exp} - \Delta H(t)_{calc})^2 \quad (6)$$

Since the relaxation toward equilibrium is solver at aging temperatures further below T_g, it is difficult to get an accurate estimate of $\Delta H(\infty)$ experimentally in the time scale of this experiment. However, Eq. (5) has been shown to overestimate $\Delta H(\infty)$ [16, 56, 57].

Table 3 Average ΔC_p values for maltose glasses aged at different temperatures measured by SDSC and MDSC

Techniques	Aging temp./ °C	ΔC_p / J g^{-1}K^{-1}
SDSC	23	0.60±0.03
SDSC	13	0.58±0.13
MDSC	20	0.62±0.04
MDSC	10	0.59±0.03

The MDSC cooled the sample at a relatively slow rate (1°C min^{-1}) and was not cooled at the faster rate (10°C min^{-1}) as were the SDSC samples because the MDSC experiment needed to be done at a slow enough rate to allow for steady state conditions and sufficient separation of the reversing (i.e. T_g) from nonreversing (i.e. enthalpic relaxation) events. Therefore, before the CF model was applied to model the enthalpic relaxation of aged maltose glasses measured by MDSC, the aging time needed to be adjusted for the quantity of time the material was below T_g, but not at the aging temperature, due to the slow cooling and heating rate used in the measurement method, as well as the equilibration time required by the MDSC method. The effective aging time is the time which the sample would need to be aged at the specific aging temperature (T_a) in order to achieve the same increase in relaxation enthalpy that occurred due to the finite heating, equilibration and cooling times. Modeling of the data without this correction would not have accounted for the aging during cooling, equilibration, and reheating. A simple addition of the amount of time that the maltose glass was below the T_g due to the aging method would not suffice, since the rate of relaxation is dependent on the distance from equilibrium [14, 34, 38, 58–60].

The calculation of the effective aging time that the 'unaged' maltose glasses were aged because of the measurement method used in MDSC is outlined below (a through d):

a) Maltose glasses were aged at different aging temperatures and times, in duplicate, until each maltose glass had developed a similar quantity of excess enthalpy (Table 4, first three columns).

b) The aging time data were normalized by dividing the time it took to develop the same relaxation enthalpy at different aging temperature (t_a) by the amount of time it took to develop the same relaxation enthalpy at 10°C (t_{10}) or 20°C (t_{20}) (Table 4, last two columns).

Table 4 Experimental data for maltose glasses aged at different temperatures used to obtain the aging time that occurred because of the MDSC measurement method

Aging temp./ °C	Aging time (t_e)/ min	Enthalpy/ J g^{-1}	$\frac{t_a}{t_{10}}$	$\frac{t_a}{t_{20}}$
10	20	4.601	1.0	0.13
15	60	4.365	3.0	0.40
20	150	4.505	7.5	1.0
25	480	4.558	24	3.2

c) The normalized aging time data were fit to an exponential function to obtain:

$$20°C \qquad y = 0.016041\,e^{(0.21053x)} \tag{7}$$

$$10°C \qquad y = 0.12434\,e^{(0.20901x)} \tag{8}$$

where y is the equivalent aging time (min) for an 'unaged' maltose glass at a single temperature, T_g onset $-x$. Thus, x is the temperature (°C) below the T_g onset of an 'unaged' maltose glass. T_g onset was used because it signifies the initial change in molecular mobility associated with the glass transition region.

d) Equations (7) and (8) were used to calculate the equivalent aging times each temperature that the material was below T_g on cooling and reheating and summed over this range to obtain the effective aging time.

The effective aging times for the MDSC experiments were found to be 93.5 and 697 min for maltose glasses aged at 20 and 10°C, respectively. It should be noted that Figs 6–8 and 9b were plotted using the actual aging time (the time the sample was held at the actual aging temperature), but could also be plotted using the adjusted aging time (the actual aging time plus the effective aging time). Since the rate of relaxation toward equilibrium is dependent on the distance from equilibrium, the effective aging time that occurred because of the MDSC measurement method would be longer for maltose glasses aged at 10°C than aged at 20°C.

The enthalpic relaxation data ($\Delta H(t)$) for the aged maltose glasses measured by SDSC and MDSC were plotted as a function of the aging time and adjusted

aging time, respectively (SDSC – Fig. 11; MDSC – Fig. 12) and were fit to Eq. (4) for each aging temperature (Solid line – Figs 11 and 12). The experimentally obtained $\Delta H(t)$ for the 10 000 min (actual aging time) aged maltose glass at 20°C as measured by MDSC was not used in fitting of Eq. (4). There was an incomplete separation of the enthalpic relaxation from the T_g observed by the secondary peak in the nonreversing heat flow that is likely due to the insufficient number of modulation cycles per glass transition region (Fig. 8). The CF model parameters obtained for aged maltose glasses measured by SDSC and MDSC are given in Table 5 and in Figs 11 and 12. These CF parameters are similar to those found by Schmidt and Lammert [16], also given in Table 5 for aged maltose glasses. The difference in CF parameters may be due to the cooling rate of 10°C min^{-1} used in this experiment compared to the quench cooling done by Schmidt and Lammert [16] as well as the slightly different aging temperature used.

Table 5 Comparison of Cowie and Ferguson [CF] model parameters obtained for aged maltose from this work and Schmidt and Lammert [16]. $\Delta H(\infty)$ was calculated using Eq. (5) and τ and β were obtained using a least squares fit of Eq. (6)

	Unaged onset/ T_g(°C)	Aging temp./ °C	$\Delta H(\infty)$/ J g^{-1}	τ/ min	β	Total sum of squares
SDSC aged at 23°C	33.80	T_g–10.8	7.33	661.1	0.44	0.3035
SDSC aged at 13°C	33.80	T_g–20.8	13.33	81039	0.32	0.6505
MDSC aged at 20°C	30.19	T_g–10.2	10.55	1254.5	0.28	0.6777
MDSC aged at 10°C	30.19	T_g–20.2	16.55	285573	0.21	0.2482
CF Parameters for aged maltose: Obtained by SDSC (a Mettler Instrument), quench cooling, and heating rate of 10°C min^{-1}						
Schmidt and Lammert [16] aged at 30°C	39.4*	T_g–9.4	7.02± 0.122** 8.1***	136.3± 15.21	0.41± 0.021	0.9141

*Obtained using unequal heating (10°C min^{-1}) and cooling (quench cool) rates. **Curve fit $\Delta H(\infty)$ and *** calculated $\Delta H(\infty)$ values

CF model parameters obtained by SDSC and MDSC in this experiment at comparable aging temperatures below T_g are not similar and the difference may be due to the aging that occurs during the MDSC method. The short aging time data at the beginning of the stretched exponential is important for curve fitting the data; however, the first $\Delta H(t)$ data point for the maltose glasses aged by MDSC is obtained at an adjusted aging time of 98.5 min (93.5 min of effective aging time +5 min of actual aging time) and 702 min (697 min of effective aging

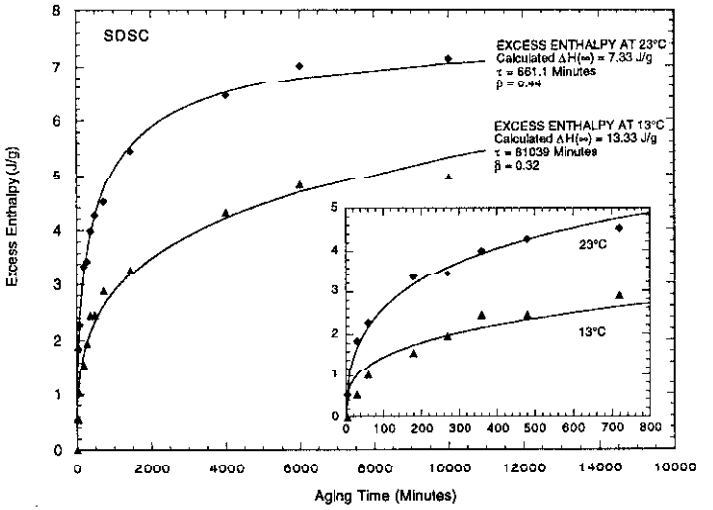

Fig. 11 Enthalpic relaxation data ($\Delta H(t)$, J g^{-1}) as a function of aging time for samples aged 5 min to 10 000 min measured by SDSC at two aging temperatures (23 and 13°C). $\Delta H(\infty)$ was calculated using Eq. (5). The solid lines are the Cowie and Ferguson model fits to the experimentally obtained excess enthalpy data points

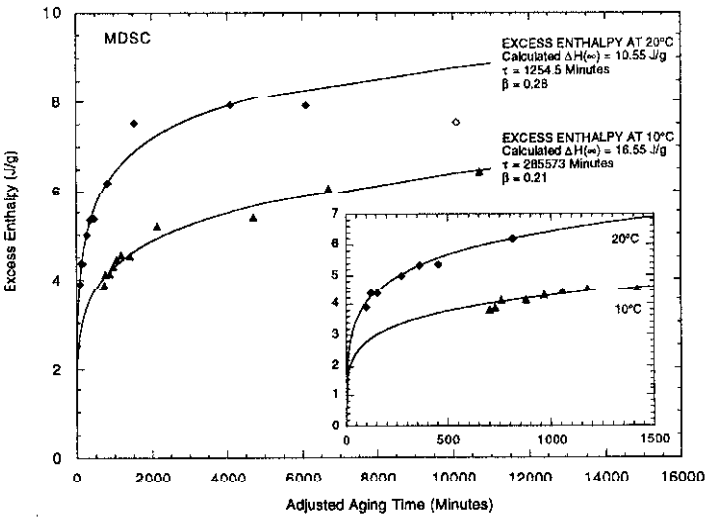

Fig. 12 Enthalpic relaxation data ($\Delta H(t)$, J g^{-1}) as a function of adjusted aging time for samples aged for 5 to 10 000 min measured by MDSC at two aging temperatures 20 and 10°C. $\Delta H(\infty)$ was calculated using Eq. (5). The solid lines are the Cowie and Ferguson model fits to the experimentally obtained excess enthalpy data points. The open diamond is the 10 000 min aging value, without time adjustment, that was not used in the CF model curve fit because there was an incomplete separation of the enthalpic relaxation from the T_g observed by the secondary peak in the nonreversing heat flow that is likely due to the insufficient number of modulation cycles per glass transition region (Fig. 8)

time +5 min of actual aging time) at aging temperatures of 20 and 10°C, respectively. The modulated heating profile used in MDSC may also have an effect on the CF parameters. Thus modeling of enthalpic relaxation data obtained by MDSC may give CF modeling parameters that are not a true representation of the relaxation of the material toward equilibrium. However, enthalpic data obtained by both SDSC and MDSC have shown that the relaxation of aged maltose glasses toward equilibrium does take longer at aging temperatures further below T_g the material is aged (Table 5) and this is similar to what occurs with other aged polymers such as fully cured epoxies [34], indomethacin, PVP, and sucrose [14], and poly(methyl methacrylate) [56].

Tool-Narayanaswamy-Moynihan (TNM) model

The Tool-Narayanaswamy-Moynihan Model (TNM Model) also uses the Williams Watts equation (Eq. (1a)) to model the development of excess enthalpy over time. Unlike the CF Model, which assumes a constant τ in $\varphi(t)$, in the TNM Model τ is dependent on both temperature and structure. This dependence is described by Eq. (9) [48, 61–63]:

$$\tau(T_a,T_f) = A\exp\left[\left(\frac{x\Delta h^*}{RT_a}\right)+\left(\frac{(1-x)\Delta h^*}{RT_f(t)}\right)\right] = A\exp\left(\frac{x\Delta h^*}{RT_a}\right)\exp\left(\frac{(1-x)\Delta h^*}{RT_f(t)}\right) \quad (9)$$

where τ is the relaxation time that is dependent on temperature and structure, A is the relaxation time at an arbitrary reference temperature, Δh^* is the activation energy (or enthalpy; [35]) that expressed the temperature dependence of relaxation times near equilibrium, R is the ideal gas constant, x ($0 \leq x < 1$) is a parameter that describes the contribution of temperature and structure to τ, T_a is the aging temperature, and $T_f(t)$ is the fictive temperature. The temperature dependence of τ in Eq. (9) is $\exp(x\Delta h^*/RT_a)$; while the structural dependence is $\exp([(1-x)\Delta h^*]/[RT_f(t)])$. As the material relaxes, the structural dependence increases with time because $T_f(t)$ decreases and therefore the τ increases with time.

The $T_f(t)$ is based on the structure or enthalpy (H) of an aged material at a time, t (Fig. 13). $T_f(t)$ can be related to enthalpy by Eq. (10) [49]:

$$T_f(t) = T_a + \frac{\delta H}{\Delta C_p} - T_a + \frac{[H(t) - H(\infty)]}{\Delta C_p} \quad (10)$$

where $H(t)$ is the enthalpy at a time, t, $H(\infty)$ is the enthalpy at $t=\infty$, and $\Delta C_p = C_{p_l} - C_{p_g}$, the change in heat capacity at the glass transition where l=liquid and g=glass. Thus, $T_f(t)$ is merely a way to convert temperature data into enthalpy data.

The Williams and Watts stretched exponential distribution of relaxation times is assumed during physical aging (Eq. (4a)), the structure and temperature de-

pendence of that relaxation can be described by the TNM model (Eq. (9)). Equations 4, 4a, 9 and 10 can be combined to obtain:

$$\Delta H(t) = \Delta H(\infty)\left[1 - \exp\left[-\left[\frac{t}{A\exp\left(\frac{x\Delta h^*}{RT_a} + \frac{(1-x)\Delta h^*}{R\left(T_a + \frac{[\Delta H(\infty) - \Delta H(t)]}{\Delta C_p}\right)}\right)}\right]^{\beta}\right]\right] \quad (11)$$

Equation (11) contains 3 measured parameters, ΔC_p, T_a and Δh^*, and one constant, R (the gas constant). ΔH(it) *vs.* aging time (t) can be plotted for any aging temperature, T_a, and fit to find the 4 adjustable parameters, A, x, $\Delta H(\infty)$, and β. These parameters can be used to describe the enthalpic relaxation of a material at a given aging temperature and these parameters for synthetic organic and inorganic materials have been recently reviewed by Hodge [64].

Equation (11) was solved for aged maltose glasses measured by SDSC and MDSC using the actual and adjusted aging time (described above) values for SDSC and MDSC experiments, respectively. $\Delta H(\infty)$ was calculated from Eq. (5) using the same parameters as described above. The A, x, and β were determined using a nonlinear least squares fit at each aging temperature for SDSC and MDSC using the solver function in Microsoft Excel. The Microsoft Excel solrer function minimized the sum of the difference between experimental and calculated ΔH values using Eq. (6). The ln$A$ was changed manually to minimize the error, since the solver had difficulty minimizing this variable with the other variables simultaneously and solver was then used to optimize for x and β.

The $\Delta h^*/R$ value was obtained experimentally using the method of Moynihan *et al.* [35]. The SDSC and MDSC unaged ΔC_p (0.60 J g^{-1} K^{-1}) for maltose glasses given in Table 2 were used. The $\Delta h^*/R$ value was found to be 78 479 K for maltose. Similar $\Delta h^*/R$ values were measured for fructose and sorbitol glasses that ranged from 72 323–96 630 K and 84 717–87 605 K, respectively [65]. Simatos *et al.* [65] determined the $\Delta h^*/R$ parameters for fructose and sorbitol glasses to examine the effect of different heating and cooling rates on the fragility parameter.

The TNM parameters calculated for aged maltose glasses measured by SDSC and MDSC are given in Table 6. The SDSC TNM parameters were not similar to the values obtained by MDSC. It is known that the further below T_g a material is aged, the longer it takes to reach equilibrium [14, 34, 38, 58–60]. Thus, the $\Delta H(\infty)$ values obtained at aging temperatures further below T_g should be greater than those that were obtained at aging temperatures closer to T_g. This was observed for aged maltose glasses measured by SDSC and MDSC.

TNM model parameters obtained for maltose glasses in this experiment are similar to parameters obtained for aged synthetic polymers reported by Hodge [64]. However, the TNM model parameters given by Hodge [64] may not have

been obtained in the same manner as the TNM model parameters for aged maltose glasses. In this experiment, the $\Delta H(\infty)$ value was calculated (using Eq. (5)), the ln$A$ was changed manually, and the x, and β were optimized for a single aging temperature; whereas, the TNM model can be solved for a single aging temperature or several different aging temperatures below T_g with all 4 parameters ($\Delta H(\infty)$, ln$A$, x and β) optimized at one time.

Table 6 Comparison of Tool-Narayanaswamy-Moynihan (TNM) model parameters obtained for aged maltose glasses measured by SDSC and MDSC. $\Delta H(\infty)$ was calculated using Eq. (5) and x and β were obtained using the solver function in Microsoft Excel by minimizing Eq. (6)

	Aging temp./ °C	$-\ln A$	$\Delta H(\infty)$	x	β	Total sum of squares
SDSC	23	257.76	7.33	0.78	0.62	0.4441
SDSC	13	261.63	13.33	0.86	0.39	0.6715
MDSC	20	259.77	10.55	0.84	0.36	1.1049
MDSC	10	264.15	16.55	0.96	0.22	0.2809

At the time this discussion was written, the TNM model had not been used to describe the physical aging of food materials. However, Shogren [20] reported that the DSC curve obtained for cornstarch (13.8% moisture; T_{max}=50°C; T_g=82°C) aged for 7 days at 22°C was similar to the DSC curve for polyvinylchloride (PVC) aged 6 days at 40°C by Hodge and Berens [66]. The TNM parameters obtained for PVC were x=0.25 and β=0.11 indicating the relaxation of PVC was more dependent on structure than on aging temperature. Shogren [20] related the TNM parameters obtained for the PVC to aging behavior of starch indicating that some type of local ordering was occurring in the moist starch. However, it is questionable whether physical aging was the phenomena being observed by Shogren [20]. At 10–20% moisture, the endothermic peak associated with physical aging was present on the DSC scan [20, 22] but at 2% moisture it was observed [22]. Yuan and Thompson [22] believe the disruption of water-starch interactions rather than physical aging is the cause of the endothermic peak observed at about 50°C.

Comparison of the CF and TNM model parameters

The β values obtained by the CF and TNM model (Tables 5 and 6, respectively) for aged maltose glasses measured by SDSC and MDSC are not similar; however, both models do show a decreasing trend in β as the aging temperature is decreased further below T_g. The CF model assumes that the τ and β are constant for a single aging temperatures below T_g, but τ and β changes with different aging temperatures below T_g; whereas the TNM model assumes the β is constant and the τ changes for different aging times and temperatures below T_g. Thus, a

comparison of the β values may not be the appropriate way to describe differences between the CF and TNM models.

The CF model can be used to describe the long time aging behavior of materials at a specific aging temperature; whereas, the TNM model can describe the aging behavior of materials at any aging time or aging temperature and can be used to predict the shape of the heat capacity *vs.* temperature for aged materials. However, there is debate in the literature regarding the appropriateness of using a constant τ in $\varphi(t)$ to describe the enthalpic relaxation of material [54, 56, 64, 67, 68], but Cowie and Ferguson [54] reported that there was no significant difference (at the 95% confidence level) between using a constant τ in $\varphi(t)$ as in the CF model or a time dependent $\tau(t)$ in $\varphi(t)$ as in the TNM model to fit enthalpic relaxation data. If the physical aging behavior of a material at one aging temperature is to be examined, the CF model may be a better choice than the TNM model; whereas, the TNM model may be a better choice than the CF model to describe the physical aging behavior of materials at several different aging temperatures below T_g.

Conclusions

SDSC and MDSC have been used to examine the changes in T_g (T_g onset, T_g midpoint, T_g endpoint, T_g calculated) and excess enthalpy that resulted from the physical aging of aged maltose glasses aged at two different temperatures below the glass transition temperature. The T_g onset, midpoint, and endpoint for aged maltose glasses increased slightly with aging time. The T_g calculated decreased for aged maltose glasses measured by SDSC whereas the T_g calculated measured by MDSC slightly increased. Maltose glasses aged at the temperature further below T_g took longer to approach equilibrium. Two mathematical models, CF and TNM, were fit to the enthalpic relaxation data of aged maltose glasses measured by SDSC and MDSC. The parameters from the CF and TNM models decreased the further below T_g the material was aged. Thus, the further below T_g the material is aged the longer it takes the material to reach equilibrium. Physical aging is a process that can occur in the lifetime of solid food materials (i.e. hard candies, low moisture foods) altering their physical properties and decreasing their shelf life. If food manufacturers had a greater understanding of the mechanism that causes physical aging, its effects (such as brittleness) could be minimized. Thus, understanding the process of physical aging has the potential to be a valuable predictive tool to more accurately assure the quality, safety, and stability of foods.

References

1 L. C. E. Struik, Physical Aging in Amorphous Polymers and Other Materials. Elsevier Scientific Publishing Company, New York 1978.
2 H. Y. Roos, Phase Transitions in Foods. Academic Press, New York 1995.

3 L. Slade and H. Levine, In Carbohydrates in Food, A. C. Eliasson (Ed.), Marcel Dekker, NY pp. 41–157, 1995.
4 Z. H. Chang and J. G. Baust, J. Non-Crystalline Solids, 130 (1991a) 198.
5 Z. H. Chang and J. G. Baust, Cryobiol., 28 (1991b) 87.
6 E. Fukuoka, M. Makita and Y. Nakamura, Chem. Pharm. Bull., 37 (1989) 2782.
7 T. R. Noel, S. G. Ring and M. A. Whittam, In The Glassy States in Foods, J. M. Blanshard and P. J. Lillford (Eds.), Nottingham University Press, Loughborough, Leicestershire.
8 F. R. Noel, S. G. Ring and M. A. Whittam, Carbohydrate Res., 212 (1991) 10944.
9 T. R. Noel, S. G. Ring and M. A. Whittam, Trends in Food Sci. & Technol., 1 (1991) 62.58 A. Agrawal, J. Polymer Sci., B Polymer Physics, 27 (1989) 1449.
10 D. Simatos and G. Blond, In Water Relationships in Food, H. Levine and L. Slade (Eds), Plenum Press, New York, NY.
11 M. T. Kalichevsky, J. M. V. Blanshard and P. F. Tokarczuk, Int. J. Food Sci. Technol., 28 (1993) 139.
12 A. M. Donald, S. C. Warburton and A. C. Smith, In The Glassy States in Foods, J. M. Blanshard and P. J. Lillford (Eds), Nottingham University Press, Loughborough, Leicestershire 1993.
13 S. J. Livings, A. M. Donald and A. C. Smith, In The Glassy State in Foods, J. M. Blanshard and P. J. Lillford (Eds.), Nottingham University Press, Loughborough, Leicestershire.
14 B. C. Hancock, S. L. Shamblin and G. Zografi, Pharmaceutical Res., 12 (1995) 799.
15 M. E. Sahagian and H. D. Goff, Thermochim. Acta, 246 (1995) 271.
16 S. J. Schmidt and A. M. Lammert, J. Food Sci., 61 (1996) 870.
17 I. A. M. Appelqvist, D. Cooke, M. J. Gidley and S. J. Lane, Carbohydrate Polymers, 20 (1993) 291.
18 M. J. Gidley, D. Cooke and S. Ward-SMith, In The Glassy States in Foods, J. M. Blanshard and P. J. Lillford (Eds), Nottingham University Press, Loughborough, Leicestershire 1993
19 M. T. Kalichevsky, E. M. Jaroszkiewicz, S. Ablett, J. M. V. Blanshard and P. J. Lillford, Carbohydrate Polymers, 18 (1992) 77.
20 R. L. Shogren, Carbohydrate Polymers, 19 (1992) 83.
21 R. L. Shogren and B. K. Jasberg, J. Environ. Polym. Degrad., 2 (1994) 99.
22 R. C. Yuan and D. B. Thompson, Carbohydrate Polymers, 25 (1994) 1.
23 J. W. Lawton and Y. V. Wu, Cereal Chem., 70 (1993) 471.
24 M. J. Richardson and N. G. Savill, Polymer, 16 (1975) 753.
25 P. S. Gill, S. R. Sauerbrunn and M. Reading, J. Thermal Anal., 40 (1993) 931.
26 A. Boller, C. Schick and B. Wunderlich, Thermochim. Acta, 266 (1995) 97.
27 D. J. Hourston, M. Song, A. Hammiche, H. M. Pollock and M. Reading, Polymer, 37 (1996) 243.
28 L. N. Bell and D. E. Touma, J. Food Sci., 61 (1996) 807, 828.
29 H. D. Goff, Pure Appl. Chem., 67 (1995) 1801.
30 J. J. Izzard, S. Ablett, P. J. Lillford, V. L. Hill and I. F. Groves, J. Thermal Anal., 47 (1996) 1407.
31 Corn Refiners Association, Inc. Standard Analytical Methods. Method E-46, 1100 Connecticut Avenue, N. W., Washingon, D. C. 20036 (1992).
32 TA Instruments. Modulated DSC compendium: basic theory and experimental considerations. TA-210. New Castle, DE (1996a).
33 B. Wunderlich, Y. Jin and A. Boller, Thermochim. Acta, 238 (1994) 277.
34 S. Montserrat, J. Polymer Sci. B. Polymer Physics, 32 (1994) 509.
35 C. T. Moynihan, A. J. Easteal, J. Wilder and J. Tucker, J. Phys. Chem., 78 (1974) 2673.
36 A. Eisenberg, Ch. 2 in Physical Properties of Polymers, 2nd Ed. ACS Professional Reference Book, American Chemical Society. Washington DC (1993).

37 TA Instruments. Universal Analysis Operator's Manual. PN 925609.002. New Castle, DE (1996b).
38 J. M. G. Cowie and R. Ferguson, Macromol., 22 (1989) 2307.
39 J. M. O'Reilly, A review of the effect of polymer structure on enthalpy recovery in glasses. In Thermal Analysis in Polymer Characterization, E. A. Turi (Ed.), Heyden, Philadelphia, PA 1981.
40 Y. Jin, J. Bonilla, Y. Lin, L. McCracken and J. Carnahan, J. Thermal Anal., 46 (1996) 1047.
41 Y. Roos, Carbohydrate Res., 238 (1993) 39.42 P. D. Orford, R. Parker, S. G. Ring and A. C. Smith, Int. J. Biol. Macromol., 11 (1989) 91
42 P. D. Orford, R. Parker, S. G. Ring and A. C. Smith, Int. J. Biol. Macromol., 11 (1989) 91.
43 J. M. Hutchinson, Prog. Polym. Sci., 20 (1995) 703.
44 C. B. McGowan, D. Y. Kim and R. B. Blumstein, Macromol, 25 (1992) 4658.
45 I. Echeverria, P. Su, S. Simon and D. Plazek, J. Polymer Sci. B Polymer Physics, 33 (1995) 2457.
46 A. R. Berens and I. M. Hodge, Macromol., 15 (1982) 756.
47 A. Aref Azar and J. N. Hay, Polymer, 23 (1982) 1129.
48 A. Q. Tool, J. Amer. Ceramic Soc., 29 (1946) 240.
49 J. J. Tribone, J. M. O'Reilly and J. Greener, Macromol., 19 (1986) 1732.
50 S. C. Jain and R. Simha, Macromol., 15 (1982) 1522.
51 J. M. G. Cowie and R. Ferguson, Polymer Communications, 27 (1986) 258.
52 G. Williams and D. C. Watts, Trans. Faraday. Soc., 66 (1970) 80.
53 J. M. G. Cowie, S. Elliott, R. Ferguson and R. Simha, Polymer Communications, 11 (1987) 298.
54 J. M. G. Cowie and R. Ferguson, Polymer, 36 (1995) 4159.
55 F. Biddlestone, A. A. Goodwin, J. N. Hay and G. A. C. Mouledous, Polymer, 32 (1991) 3119.
56 J. M. G. Cowie and R. Ferguson, Polymer, 34 (1993) 2135.
57 J. L. Gomez Ribelles, A. Ribes Greus and R. A. Diaz Calleja, Polymer, 31 (1990) 223.
58 A. Agrawal, J. Polymer Sci., B. Polymer Physics, 27 (1989) 1449.
59 A. Aref-Azar, F. Arnoux, F. Biddlestone and J. N. Hay, Thermochim. Acta, 273 (1996) 217.
60 H. Yoshida, Thermochim. Acta, 266 (1995) 119.
61 R. Gardon and O. S. Narayanaswamy, J. Amer. Ceramic Soc., 53 (1970) 380.
62 O. S. Narayanaswamy, J. Amer. Ceramic Soc., 54 (1971) 491.
63 C. T. Moynihan, A. J. Easteal, M. A. DeBolt and J. Tucker, J. Amer. Chem. Soc., 59 (1976) 12.
64 I. M. Hodge, J. Non-Crystalline Solids, 169 (1994) 211.
65 G. Simatos, G. Blond, G. Roudaut, D. Champion, J. Perez and A. L. Faivre, J. Thermal Anal., 47 (1996) 1419.
66 I. M. Hodge and A. R. Berens, Macromol., 15 (1982) 762.
67 S. Z. D. Cheng, Polymer, 33 (1992) 4884.
68 I. M. Hodge and J. M. O'Reilly, Polymer, 33 (1992) 4883.